ALTERNATIVE ABRASIVES FRAGMENTATION EFFECT DURING THE AWJ FORMING PROCESS

ANDRZEJ PEREC[1],
ELZBIETA KAWECKA[1],
ALEKSANDRA RADOMSKA-ZALAS[2],
MAGDALENA KRAKOWIAK[1]

[1]Jacob of Paradies University, Faculty of Technology, Gorzow Wielkopolski, Poland,

[2]Gorzow Center of Technology, Scientific and Technology Park, Gorzow Wielkopolski, Poland

DOI: 10.17973/MMSJ.2026_06_2026051

e-mail to corresponding author: aperec@ajp.edu.pl

The effects of high-pressure abrasive water jet (AWJ) machining strongly depend on the dimensions and distribution of the abrasive grains. This study explores how abrasives break down during the generation of AWJ operations. Following formation in the cutting head, the abrasive material's grain size was measured, and the Folk and Ward technique was used to assess grain distribution. Grain distribution was examined first concerning the various abrasive grain concentrations in the jet, such as alumina, ilmenite, and industrial glass. The recovery analysis was also conducted for each tested abrasive material, and the recycling factor was calculated. The recovery analysis was also conducted for each tested abrasive material, and the recycling factor was calculated.

KEYWORDS
abrasive grain disintegration, alumina, ilmenite, crushed glass

1 INTRODUCTION

Since the abrasive grain size distribution determines the effectiveness of most abrasive cutting processes [Kacalak et al. 2021], especially in abrasive water jet [Perec, Radomska-Zalas 2019], [Praźmo et al. 2025], it is wise to conduct in-depth research into this area to attain its maximum efficiency [Hashish 2024], [Kawecka 2024], [Perec et al. 2025a], as in the case of optimizing this process [Perec et al. 2024a], [Perec et al. 2025b].

The abrasive grains' dimensions and shape have a significant impact on abrasive machining processes [Nadolny et al. 2017], [Kukielka et al. 2005] for achieving a great precision and efficiency [Krolczyk et al. 2021], [Kukielka, Kustra 2003], [Grochala et al. 2019] of the treated surface.

Intensive abrasive consumption impacts the properties and AWJ-machined costs of products [Jerman et al. 2015], [Prazmo et al. 2017], particularly at difficult-to-machine materials [Radomska-Zalas 2023], [Szatkiewicz et al. 2023], [Perec, Musial 2021]. Recycling may significantly reduce abrasive material expenses.

The intensive abrasive material disintegration [Hloch et al. 2018], [Lehocka et al. 2020] occurs during the grains' injection into the jet in the mixing chamber and the focusing tube inside the cutting head. It is the characteristic properties of the jet forming process [Riha et al. 2021], because abrasive grain size distribution is essential to the effectiveness of most abrasive cutting processes. This phenomenon was the subject of research in various research centers.

A garnet abrasive recycling outcomes in aluminum AWJ cutting were published by Chetty et al. [Kantha Babu, Krishnaiah Chetty 2003]. Grain size, cutting depth, cutting breadth, and cutting taper are all impacted by pressure, feed rate, and abrasive flow rate. Using recycled abrasives improved the cut surface quality. Additionally, the cut slot taper was decreased. These impacts demonstrate that choosing the right abrasive particle size distribution is crucial to achieving superior outcomes.

Whereas Hlavac et al., [Hlaváč et al. 2010] determined the degree of particle size changes produced in the cutting head and agreed that understanding the grain size at the cutting head output is essential for researching other phenomena, like the water stream's impact with industrial mineral particles on a solid-state object or its effect on the fluid barrier or reverse flow of the same kind.

Aydin et al. [Aydin 2014] examined the abrasive properties of their recycling in AWJ cutting. Since these abrasives may be efficiently recycled for rock-cutting, a mass of abrasive grain exceeding 106 µm, was regarded as the performance requirement in abrasive recycling. According to the results, the fragmented abrasive particle parts were still usable. Additionally, recycled garnet abrasive materials [Aydin 2015] were subject to research on the maximal cutting efficiency achievement under the following variable control parameters: depth of cut, kerf breadth, kerf tilt angle, and roughness of the kerf lateral surface. After catching, drying, and sieving, following each pass, the grain sizes of garnet lower than 106 µm were disqualified. Many of the spent abrasives were suitable for use in the cutting process. After the first pass, the recycling factor of abrasives was more than 81%, and after the fourth pass, it was 17%.

The research of Hreha et al. [Hreha et al. 2015] shows that the vibration emission frequency during cutting is directly determined by the abrasive mass flow rate. A more thorough physical model of how different abrasive characteristics affect jet formation and real-time process monitoring might be obtained by correlating your fragmentation data with these vibration spectrum shifts, where larger flow rates move peaks toward higher frequency zones.

Particle disintegration in the abrasive water jet technique was studied by Zaremba et al [Zaremba et al. 2015]. The goal was to gain a deeper understanding of the material removal process during AWIJ machining. In a pressure range of 250 to 550 MPa, micro- and macro-cutting systems that reflect the current state of the art were employed. For abrasive number load ratios, the particle disintegration was examined. The jet generating step is where the greatest particle amount disintegration occurs. Disintegration may occur in the focusing tube cylinder, the focusing tube intake guiding cone, or the mixing chamber. Determining the disintegration ratio in these locations is difficult. Delivery of the abrasive in the jet direction may decrease disintegration in the mixing tube and intake cone.

To determine how garnet's rate, physical characteristics, and particle size distribution affect rock-cutting effectiveness, Gye-Chun Cho et al. [Oh et al. 2019] conducted a study using garnet materials. The abrasive water jet was also evaluated for garnet grain disintegration. The test findings showed that the main determinants of rock-cutting efficiency are density, hardness, garnet purity, and grain size distribution.

An experimental study on the effect of the cutting head interior form on the grain fragmentation degree in the AWJ creation process concerning reverse jet disintegration of materials was conducted by Hlavac et al. [Hlavac et al. 2008].

Based on observing abrasive breakage characteristics, Cui [Cui et al. 2025] suggested a numerical model that uses the Split Hopkinson Pressure Bar (SHPB) to forecast grain disintegration characteristics. The experimental findings showed a 14.1% decrease in the abrasive grain size without affecting the distribution function. The numerical results of the abrasive grain collisions happen in the nozzle's tangential and convergent regions. The study's conclusions provide a solid framework for abrasive recycling and the nozzle design concept.

Gembalová et al.'s publication [Gembalová et al. 2021] focuses on a critical examination of some of the findings of earlier published research about the relationship between the quantity of interacting particles and the acoustic emissions recorded on cut materials. By examining the kerf walls created by the Abrasive Water Jet (AWJ), the study sought to understand how abrasive grains changed after contact with metals. The abrasive grain size following the mixing procedure and variations in this size during contact with the target material were the focus of the discussion.

The abrasive material recycling of abrasive suspension jet (ASJ) was evaluated by Ma et al. [Ma et al. 2021]. The recycled abrasives retain their powerful cutting capacity even after the large particle impurities are sieved away. Abrasive material can be fully utilized, and the cutting process can maintain the same performance when, during each reuse, it is recharged to 30% in each cycle. Abrasive grains between 90 and 180 µm are best for cutting because they cause better surface roughness when compared to bigger abrasives at high efficiency.

Reusing abrasive grains in abrasive water jet cutting was proposed by Krajcarz and Spadlo [Krajcarz, Spadło 2017]. The new abrasive garnet #120 is made from the disintegration particles of garnet #80. Fresh and recycled garnet #120 was used to cut the aluminum alloy to assess its capacity to cut recyclable abrasive grains. The assessment of surface geometrical structure was the main focus of the experimental investigation of cutting surface quality.

In the AWJ machining process, the abrasive interacts with the focusing tube and then with the workpiece. Previous research [Prazmo et al. 2017] has shown that the highest disintegration, at 70%, occurs during jet formation, while in the cutting of various materials, further defragmentation does not exceed 10%. Therefore, this study examined the fragmentation stage, which has the greatest impact.

The state-of-the-art analysis shows that abrasive grain fragmentation studies were the subject of research in many scientific centers. Generally, these studies were used to determine the reusability of an abrasive that had already been used once. However, the analyses were conducted for the most popular abrasive, garnet, originating from various deposits.

Garnet's abrasive prices in the global markets are volatile, and there is a risk of supply disruption. Research into alternative abrasives and their potential recycling contributes to filling this research gap, which is the purpose of this article. The research's main objective and uniqueness are the influence of the alternative (non-garnet) abrasive flow rate on its disintegration during the AWJ process formation. This topic was presented in earlier published papers [Perec 2017] and [Perec 2021], in a limited scope only, and this work was expanded upon.

2 MATERIALS AND METHODS

Garnet is the most often utilized abrasive in AWJ systems [Perec 2011] and [Praźmo et al. 2025] in the wide pressure range of 400 to 600 MPa. Its special qualities (Table 1) allow it to achieve high performance with comparatively low focusing tube wear, which is why it is commonly adopted in these processes [Hreha et al. 2014].

Crystallographic system	Cubic
Unit cell	a = 11.53 Å
Mohs hardness	6.5-7.5
Density	4.1-4.3 kg/dm^3
Fracture	Conchoidal to uneven
Color	Deep red to reddish-brown, sometimes with a violet or brown

Table 1. Garnet's basic characteristics

Since the primary expense of processing an AWJ is the cost of abrasives [Nag et al. 2018], [Perec et al. 2024b], deliberate efforts are made to employ and recycle the least expensive abrasive materials. The primary reason for choosing corundum and ilmenite was to test abrasive materials with opposite properties. On the other hand, Crushed glass was selected for ecological/economic reasons, as the garnet cost represents over 60% of the total processing cost.

2.1 Alumina

The alumina abrasive material is stable and hard. After diamond, it is the second-hardest natural mineral. Acids and the alkaline surroundings do not react with it. The natural corundum comes into composition with valuable stones like rubies, sapphires, and metamorphic rocks, like emery. Transparent and emerald are the two most prevalent alumina types.

Many alumina abrasives are easily synthetically produced. Abrasive grains come in a range of purities and chemical composition grades. In sandblasting, one can use industrial abrasive materials based on alumina, but the use of alumina abrasive in water-abrasive jet cutting (AWJ) is limited by the nozzles' rapid wear and the several abrasive size fractions with varying mineralogic and chemical cleanliness of alumina-based abrasives. The fundamental characteristics of corundum are presented in Table 2.

Crystallographic system	Trigonal (pseudohexagonal)
Unit cell	a = 4.76 Å; c = 12.99 Å
Mohs hardness	9.0
Density	4,0 - 4,1 kg/dm^3
Fracture	Shell
Color	various colors, as blue, red, purple, pink, green, yellow, orange, gray, brown, black, white, and even colorless,

Table 2. Alumina basic characteristics

Alumina abrasive has good recycling potential [Perec et al. 2019]. Recycling remains inexpensive for synthetic corundum. It is a secondary raw material - a recycled product from waste under abrasive tool production. In the tests, BFA synthetic alumina was used. BFA alumina is brown aluminum oxide made from bauxite and other raw materials. Alumina is renowned for its excellent strength and high hardness. High tensile strength metals, including carbon steel, hard alloy, annealed malleable cast iron, and general-purpose alloy steel, may be ground using tools constructed from this abrasive. Additionally, alumina can be used as a refractory material. It is also frequently found in coated abrasive instruments, particularly for metal grinding. Dengfeng Sweet Abrasives Co., Ltd., situated in Dengfeng City,

Zhengzhou, Henan, China, manufactures the corundum utilized in this study.

Its properties are listed in Table 3, and the grain size distribution is shown in Figure 1.

Feature	Values	
Chemical composition	Al_2O_3	94.5÷95.5 %
	SiO_2	1.33÷1.50 %
	Fe_2O_3	0.18÷0.30 %
	Ti_2O	2.45÷3.50 %
	CaO	0.11÷0.30 %
Melting point	2050 ˚C	

Table 3. BFA alumina abrasive properties

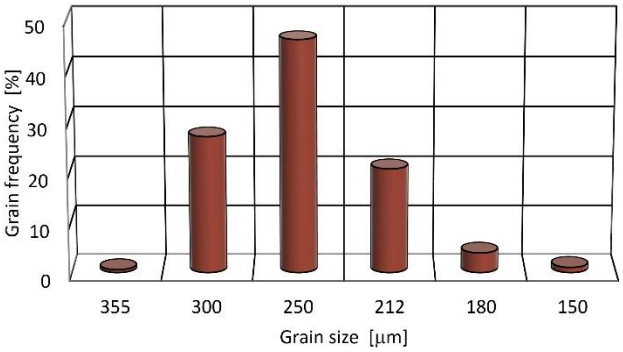

Figure 1. BFA60 alumina abrasive grain distribution

2.2 Ilmenite

Ilmenite ($FeTiO_3$) is a titanium–iron oxide mineral that typically appears black or dark gray. It represents the primary source for industrial production of titanium dioxide pigments, which are widely used in paints, plastics, paper, and coatings. Geologically, ilmenite often crystallizes early from magmas and, because of its high density, tends to accumulate in lower layers during magmatic differentiation. It also occurs in placer deposits, frequently associated with other heavy minerals such as garnet, rutile, and zircon. Commercially, ilmenite is extracted from bedrock deposits and from mineral sands across various regions worldwide, including Australia, Brazil, Russia, Canada, and several Asian and African countries [Martinec et al. 2002].

Ilmenite also occurs in heavy sedimentary rocks (the black fraction of sands), In this form it is mined on all continents, in Europe (Norway, Russia), Asia (China, India, Malaysia, Sri Lanka, Thailand), Africa (Sierra Leone, South Africa), both Americas (Brazil, Canada, United States), and the Australia, as ilmenite sand in heavy fractions in river or fluvial sand (together with garnets, staurolite, etc.) or as massive or granular ilmenite in the bedrock, together with rutile, magnetite, zircon, etc. [Martinec et al. 2002]. The research used the ilmenite abrasive produced by GMA Garnet Australia, which is available under the trade name New Steel. In the case of this producer, ilmenite is a waste product obtained during the process of producing alluvial garnet, accompanying garnet deposits. Ilmenite separation is often carried out in a magnetic field because ilmenite is weakly magnetic and can be easily separated from non-magnetic minerals such as garnets.

Additional characteristics of this abrasive are shown in Table 4. The grain size distribution is presented in Figure 2. The largest percentage share, over 33%, belongs to the fraction with a grain size of 150 µm.

Crystallographic system	Hexagonal
Unit cell	a = 5.09 Å; c = 14.09 Å
Mohs hardness	5.0-6.0
Density	4.5-5.0 kg/dm^3
Fracture	Shell to uneven
Color	Steel-black

Table 4. Ilmenite basic characteristics

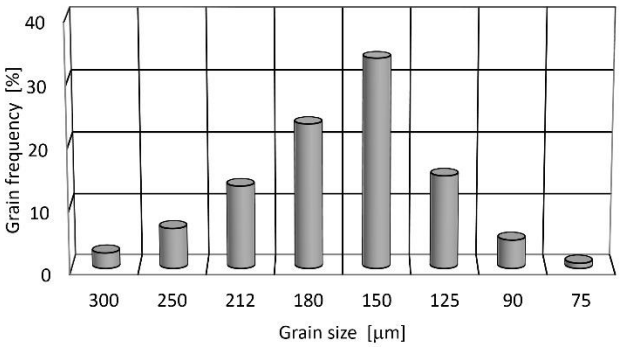

Figure 2. NS90 ilmenite abrasive grain distribution

2.3 Crushed glass

Abrasives produced from crushed soda–lime (Na–Ca) glass are among the most common recycled glass materials. They are typically obtained from industrial by-products or post-consumer waste glass that has been sorted and processed. While these abrasives are not standard in abrasive water jet (AWJ) cutting applications, they are often introduced in experimental studies because of their availability, low cost, and environmental neutrality. However, due to their brittle nature, their usefulness is limited to softer materials rather than hard metals or rock substrates *[Martinec et al. 2002]*. Due to their brittle nature, Na-Ca glass-based abrasives are ineffective in cutting thick rocks and steel cases. Only soft materials like rubber, plastic, and wood should be sliced with this abrasive. The dust produced as a processing result is environmentally neutral *[Martinec et al. 2002]*.

Abrasive materials derived from high-density industrial glass (SPDG60) offer more application opportunities. The experiments were conducted using this abrasive material, characterized in Table 4. The fraction with grain sizes between 212 µm and 250 µm characterized the biggest percentage share of the examined grain population (Figure 3).

Crystallographic system	amorphous
Mohs hardness	5.0
Density	3.6-3.8 kg/dm^3
Fracture	Shell-like, very sharp, sword-shaped grains
Color	Deep-brown, deep-gray, black.

Table 5. SPDG glass basic characteristics

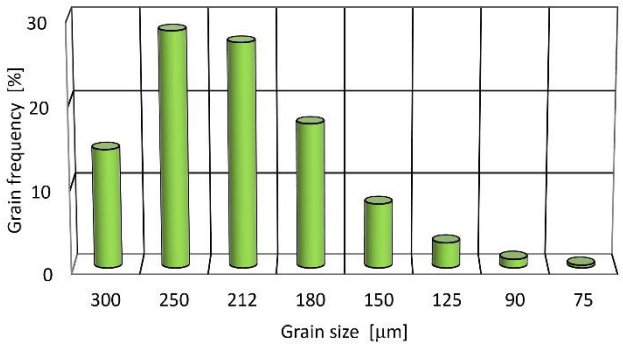

Figure 3. SPDG60 glass abrasive grain distribution

2.4 Test stand

The devices used in the test were an intensifier type I50 by KMT Waterjet Systems Inc., USA, and a CNC table type ILS55 by TECHNI Waterjet, Australia, with a dedicated PC control system.

The study was carried out under 390 MPa of pressure, utilizing two sets of cutting heads:

- 0.25 mm ID water nozzle/0.76 mm ID focusing tube
- A focusing tube with a 1.02 mm ID and a 0.33 mm ID water nozzle.

The amount of abrasive in the jet was the variable control parameter. For the testing, the following values were chosen: 15%, 17.5%, 20%, 22.5%, and 25%.

A special tank was used to catch the abrasive material as it left the cutting head. Its job is to gather the material and keep it from disintegrating once it leaves the cutting head. To prevent the bottom of the PVC catcher from perforating, a steel cover was placed over it (Figure 4).

The Retsch sieve analyzer was used for the abrasive particle size distribution tests. The digital scales were used to weigh the mass of abrasive that remained on the sieves five times, and the average of these readings was computed.

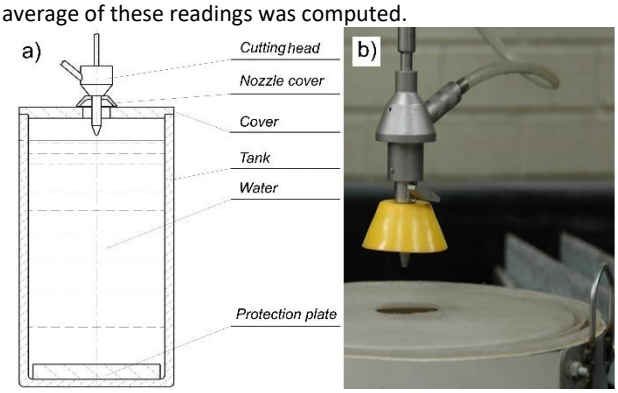

Figure 4. Special abrasive particle collector; a) cross-section, b) upper area view

3 RESULTS

3.1 BFA60 alumina grains disintegration

With a jet created in a head with a 0.25 mm diameter water nozzle and a 0.76 mm diameter water-abrasive nozzle under 390 MPa of pressure, the results of the BFA60 abrasive fragmentation test are shown in Figure 5.

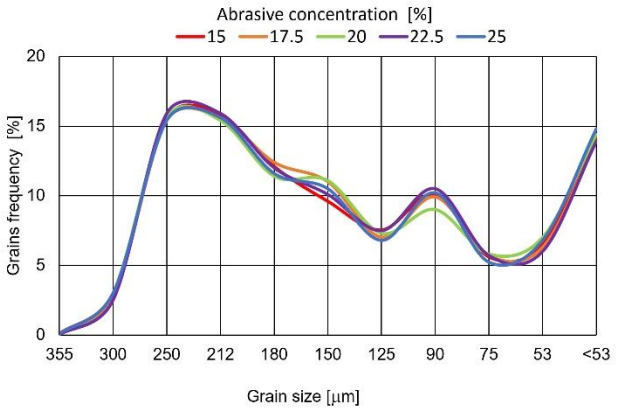

Figure 5. BFA60 alumina grains fragmentation following passage through a cutting head with the 0.25 mm water nozzle and the 0.75 mm focusing tube

The 250 µm and 212 µm fractions are likewise the most common in this distribution, accounting for more than 17% of the total. At nearly 15% of the total, the abrasive fraction with dimensions smaller than 53 µm has the second-highest proportion, followed by the 90 µm fraction, which has a value close to 10%. In this case, the abrasive grain size was also reduced. Grain fragmentation was not significantly affected by the flow rate of the abrasive material (the quantity of abrasive in the jet) within the studied range.

Figure 6 displays the outcomes of the BFA60 abrasive fragmentation test with a jet formed in a head with a 0.33 mm diameter water nozzle and a 1.00 mm diameter water-abrasive nozzle at a pressure of 390 MPa. The distribution is remarkably similar to that discussed earlier. With a proportion of over 17% each, the 250 µm and 212 µm fractions are also the most prevalent in this instance. The abrasive with dimensions less than 53 µm has the second greatest percentage, accounting for over 15% of the total. A reduction in the size of the abrasive grains was also seen in this instance. In the measured range, the abrasive material's flow rate (amount of abrasive in the jet) had no discernible influence on grain disintegration.

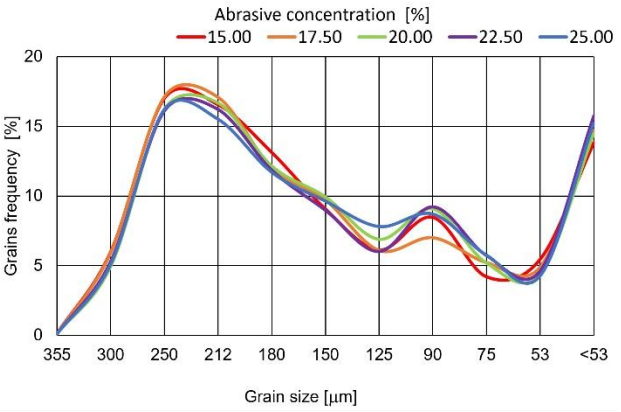

Figure 6. BFA60 alumina grains fragmentation following passage through a cutting head with the 0.33 mm water nozzle and the 1.00 mm focusing tube

3.2 NS90 ilmenite grains fragmentation

Figure 7 displays the findings of the NS90 ilmenite abrasive fragmentation test, in the jet, generated at 390 MPa of pressure in the cutting head with a 0.25 mm water nozzle and a 0.75 mm water-abrasive nozzle.

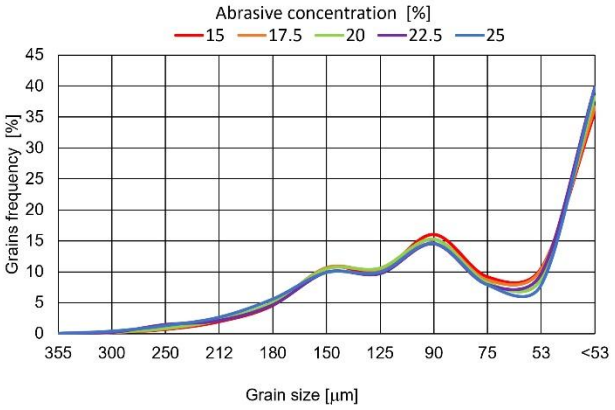

Figure 7. NS90 ilmenite grains fragmentation following passage through a cutting head with the 0.25 mm water nozzle and the 0.75 mm focusing tube

Grain sizes less than 53 µm were the biggest percentage, equal to around 38% of the total grain population. Grain sizes of 90 µm characterized the second greatest percentage, with a share of around 15%. Overall, a significant reduction in particle size was observed. Grain fragmentation is not significantly impacted by the abrasive material's flow rate (concentration of the abrasive in the jet) within the studied range.

Figure 8 shows the results of the NS90 ilmenite abrasive fragmentation test during the production of a jet at a pressure of 390 MPa in a head with a 0.33 mm diameter water nozzle and a 1.00 mm diameter water-abrasive nozzle.

The biggest percentage, equivalent to 40%, corresponds to the fraction of grains smaller than 53 µm. The 90 µm-sized grain fraction, about 20% of the share, was the second largest. Here, a significant drop in particle size was also noted. Grain fragmentation is barely impacted by the abrasive material's flow rate (abrasive concentration in the jet) within the measured range.

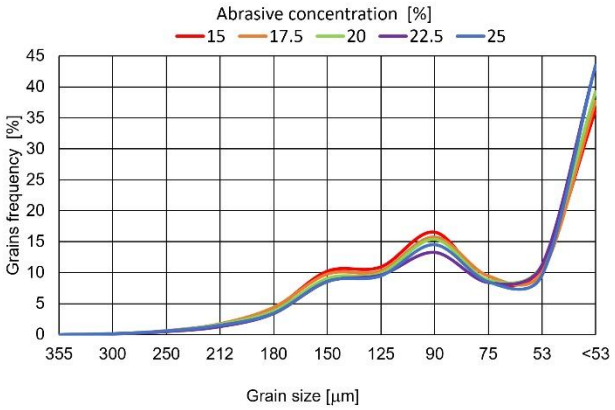

Figure 8. NS90 ilmenite abrasive fragmentation following passage through a cutting head with the 0.33 mm water nozzle and the 1.00 mm focusing tube

3.3 SPDG60 glass grains fragmentation

An SPDG60 abrasive grain fragmentation test finding, displayed in Figure 9, was made by the jet at 390 MPa of pressure in a head that had a 0.25 mm diameter water nozzle and a 0.75 mm diameter water-abrasive nozzle. The fraction of grains smaller than 53 µm takes the highest share (about 27%).

The second biggest fraction, about 90 µm grain sizes, was constituted of over 15% distribution, followed by the 150 µm fraction with a value slightly below 15%. Overall, a notable reduction in particle size was noted. Grain fragmentation is not significantly impacted by the abrasive material's flow rate (concentration of the abrasive in the jet) within the studied range.

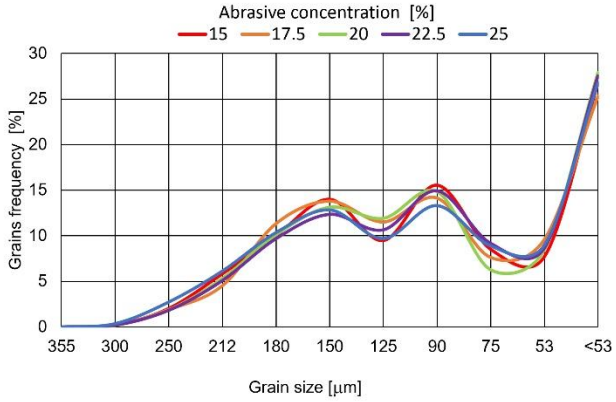

Figure 9. SPDG60 glass abrasive fragmentation following passage through a cutting head with the 0.25 mm water nozzle and the 0.75 mm focusing tube

Figure 10 shows the results of the SPDG60 abrasive fineness test while forming a jet at a pressure of 390 MPa in a head with a 0.33 mm diameter water nozzle and a 1.00 mm diameter water-abrasive nozzle. The particles smaller than 53 µm account for the highest percentage, surpassing 25%. At over 15%, the 90 µm grain size fraction was the second biggest proportion. In this instance, a notable reduction in particle size was also seen. Grain fragmentation is little impacted by the abrasive material's flow rate (concentration in the jet) within the studied range.

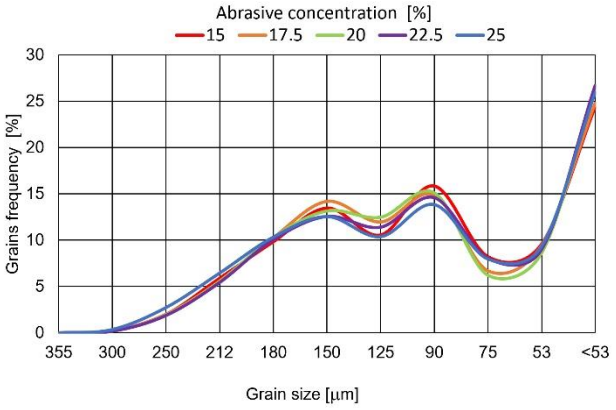

Figure 10. SPDG60 glass abrasive fragmentation following passage through a cutting head with the 0.33 mm water nozzle and the 1.00 mm focusing tube

3.4 Abrasive grain recycling

The recycling factor was determined by dividing the mass of abrasive grains after grinding and within the original size range by the mass of grains before fragmentation, according to the equation:

$$R_p = \frac{m_w}{m_p} \quad (1)$$

Where:

R_p is the recycling factor,

m_w is the grain's mass in the input size range after fragmentation,

m_p is the mass of abrasive grains before fragmentation.

This factor interpretation is simple. It describes how much of the recovered abrasive can be reused in the process again.

Following the acquisition and abrasive drying, sieve analysis was performed, and the mass of each fraction was determined. The abrasive size range for all investigated materials falls between 350 and 90 µm. All fractions less than the lower limit of the particle distribution were eliminated as ineffective in the cutting process to determine what percentage of the original range is present in the jet created in the cutting head.

Figure 11 shows the specific outcomes for each tested abrasive.

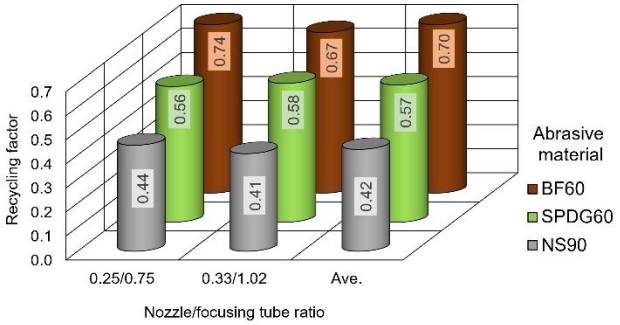

Figure 11. Recycled factors for tested abrasive materials

For the BF60 alumina abrasive, the average recycling factor was 0.7 for both water nozzle/focus tube combinations. For NS90 ilmenite, this factor is only 0.42. This is due to the relatively high fineness of this material in both combinations of water nozzle/focus tube ratios. In the SPDG60 glass abrasive case, the average recycling factor was 0.57.

3.5 Discussion

The experimental results demonstrate a clear correlation between the physical abrasive properties and their susceptibility to fragmentation during the jet-forming process. Alumina showed the highest resistance to disintegration due to its superior hardness. This behavior aligns with models of breakage mechanics in brittle materials, where microcracking under high-velocity impact leads to rapid particle comminution [Cil et al. 2020].

Differences in the behavior of a jet during jet formation are directly related to the kinetic energy of the abrasive grain accelerated to the jet velocity, as noted by Varga et al., [Varga et al. 2023] in the case of the raw materials transport. If abrasive grains of similar size accelerate to similar speeds, the kinetic energy is determined by the grain mass. This is reliable with the results of the study by Hwang et al., [Hwang et al. 2024]. The mass for particles of similar dimensions depends on the density of the abrasive material. For denser materials, such as garnets, the kinetic energy will naturally be greater than for glass.

The second factor determining fragmentation ability is dynamic brittleness. Dynamic brittleness, or brittleness under impact/dynamic loading, describes the susceptibility of material grains to cracking and fragmentation under rapid loading (e.g., impact, high pressure in mills or impact crushers). The higher the dynamic brittleness, the more easily the grain breaks into smaller fragments, creating a new surface. Glass grains are characterized by the highest dynamic brittleness; they break easily upon impact, have low energy for crack initiation and propagation, and fracture very rapidly. Ilmenite is characterized by medium dynamic brittleness, breaking more easily than corundum but more difficult than glass. Corundum has the lowest dynamic brittleness; its grains require the most energy to break, and it is the most resistant to dynamic loads similar to abrasive grains in high-speed grinding wheels [Pavloušková et al. 2020].

The abrasive grain size distribution shows a significant difference in alumina abrasive particle size distribution from that of other abrasive materials. The disintegration of alumina grains is relatively small. This is primarily due to the highest hardness and the abrasive grain's high density. The breakage of abrasive materials with lower hardness and density is significantly greater. These observations are consistent with previously published research for other abrasive materials, such as fayalite [Perec 2018] or recycled garnet [Perec 2021].

4 CONCLUSIONS

The paper quantitatively proves that recycling factors are the dominant parameters for total process economy, often much more important than the simple purchase price. Choosing the abrasive with the right recycling factor for your typical materials can easily cut abrasive-related costs by 30–70 %.

According to the testing, abrasive grain breakup and significant size reduction occurred during the cutting head's jet creation. This is typically seen as an undesirable phenomenon. It is important to note that the degree and type of abrasive grain disintegration are not significantly impacted by the abrasive concentration in the jet, which ranges from 15% to 25%. A 20-25% preponderance was seen on the grains below 53 µm for alumina abrasives that disintegrated at all concentration levels.

For all other abrasives, similar effects of grain disintegration for each concentration value were observed, and the higher predominance of grains below 53 µm dimension at the 30% level was noted.

An additional benefit is the possibility of reusing the abrasive materials as a full-fledged product.

Based on the research, the following detailed conclusions were drawn:

- Grain predominance below 53 µm is greater and equals 30% for all other abrasives, which disintegrated at each concentration value.
- The potential to reuse the abrasive ingredients as a worthwhile product is a further advantage. The following thorough findings were extracted from the research:
- For the BF60 alumina abrasive, the largest average recycling factor is 0.7.
- -The average recycling factor for NS90 ilmenite is 0.42.
- -SPDG60 glass abrasive has an average recycling factor of 0.57.

Increased particle disintegration affects both the focusing tube's lifespan and cutting performance.

This can assist in addressing the buildup issues caused by the large number of abrasives produced by waterjet cutting in landfills.

The impact of abrasive grains created in the AWJ cutting head on shape change will then be the focus of a further study.

REFERENCES

[Aydin 2014] Aydin, G. “Recycling of abrasives in abrasive water jet cutting with different types of granite,” *Arabian Journal of Geosciences*, Vol. 7, No. 10, pp. 4425–4435, 2014. DOI: 10.1007/s12517-013-1113-0.

[Aydin 2015] Aydin, G. “Performance of recycling abrasives in rock cutting by abrasive water jet,” *Journal of Central*

South University, Vol. 22, No. 3, pp. 1055–1061, 2015. DOI: 10.1007/s11771-015-2616-5.

[Cil et al. 2020] Cil, M. B. et al. "An Integrative Model for the Dynamic Behavior of Brittle Materials Based on Microcracking and Breakage Mechanics," *Journal of Dynamic Behavior of Materials*, Vol. 6, No. 4, pp. 472–488, 2020. DOI: 10.1007/s40870-020-00251-x.

[Cui et al. 2025] Cui, J. et al. "Abrasive breakage characteristics and prediction in abrasive water jets within nozzle internals," *Powder Technology*, Vol. 458, pp. 120971, 2025. DOI: 10.1016/j.powtec.2025.120971.

[Gembalová et al. 2021] Gembalová, L. et al. "Notes on the Abrasive Water Jet (AWJ) Machining," *Materials*, Vol. 14, No. 22, pp. 7032, 2021. DOI: 10.3390/ma14227032.

[Grochala et al. 2019] Grochala, D. et al. Analysis of Surface Geometry Changes after Hybrid Milling and Burnishing by Ceramic Ball, *MATERIALS*, 2019. DOI: 10.3390/ma12071179.

[Hashish 2024] Hashish, M. "Abrasive Waterjet Machining," *Materials*, Vol. 17, No. 13, pp. 3273, 2024. DOI: 10.3390/ma17133273.

[Hlavac et al. 2008] Hlavac, L. et al. "Potential of liquid jets for preparation of micro and nano particles," In Muir, A. (ed.), *Green Chemistry & Engineering Proc.*, BHR Group, Albany, New York, 2008, pp. 205–218.

[Hlaváč et al. 2010] Hlaváč, L. M. et al. "Comminution of material particles by water jets — Influence of the inner shape of the mixing chamber," *International Journal of Mineral Processing*, Vol. 95, No. 1–4, pp. 25–29, 2010. DOI: 10.1016/j.minpro.2010.03.003.

[Hloch et al. 2018] Hloch, S. et al. "Strengthening Effect after Disintegration of Stainless Steel Using Pulsating Water Jet," *Tehnički vjesnik*, Vol. 25, No. 4, pp. 1075–1079, 2018. DOI: 10.17559/TV-20170327134630.

[Hreha et al. 2014] Hreha, P. et al. "Monitoring of focusing tube wear during abrasive waterjet (AWJ) cutting of AISI 309," *Metalurgija*, Vol. 53, No. 4, pp. 533–536, 2014.

[Hreha et al. 2015] Hreha, P. et al. "Determination of vibration frequency depending on abrasive mass flow rate during abrasive water jet cutting," *The International Journal of Advanced Manufacturing Technology*, Vol. 77, No. 1–4, pp. 763–774, 2015. DOI: 10.1007/s00170-014-6497-9.

[Hwang et al. 2024] Hwang, H.-J. et al. "Semi-empirical model for abrasive particle velocity prediction in abrasive waterjet based on momentum transfer efficiency," *Computational Particle Mechanics*, Vol. 11, No. 6, pp. 2701–2713, 2024. DOI: 10.1007/s40571-024-00747-6.

[Jerman et al. 2015] Jerman, M. et al. "The Study of Abrasive Water Jet Cutting Front Development using a Two-Dimensional Cellular Automata Model," *Strojniški vestnik – Journal of Mechanical Engineering*, Vol. 61, No. 5, pp. 292–302, 2015. DOI: 10.5545/sv-jme.2014.2179.

[Kacalak et al. 2021] Kacalak, W. et al. "Assessment of the classification ability of parameters characterizing surface topography formed in manufacturing and operation processes," *Measurement*, Vol. 170, pp. 108715, 2021. DOI: 10.1016/j.measurement.2020.108715.

[Kantha Babu, Krishnaiah Chetty 2003] Kantha Babu, M. and Krishnaiah Chetty, O. V. "A study on recycling of abrasives in abrasive water jet machining," *Wear*, Vol. 254, No. 7–8, pp. 763–773, 2003. DOI: 10.1016/S0043-1648(03)00256-4.

[Kawecka 2024] Kawecka, E. "The use of metaheuristic optimization algorithm in abrasive water jet machining of white marble," *AIP Conference Proceedings*, Vol. XIV International Conference Electromachining 2023, pp. 020015, 2024. DOI: 10.1063/5.0203448.

[Krajcarz, Spadło 2017] Krajcarz, D. and Spadło, S. "Reuse of abrasive particles in abrasive waterjet cutting," *Mechanik*, No. 1, pp. 62–63, 2017. DOI: 10.17814/mechanik.2017.1.13.

[Krolczyk et al. 2021] Krolczyk, G. et al. 3D Parametric and Nonparametric Description of Surface Topography in Manufacturing Processes, *Materials*, 2021. DOI: 10.3390/ma14081987.

[Kukielka et al. 2005] Kukielka, L. et al. Numerical analysis of states of strain and stress of material during machining with a single abrasive grain, *Computer Methods And Experimental Measurements For Surface Effects And Contact Mechanics VII*, 2005.

[Kukielka, Kustra 2003] Kukielka, L. and Kustra, J. Numerical analysis of thermal phenomena and deformations in processing zone in the centerless continuous grinding process, *Surface Treatment VI: Computer Methods And Experimental Measurements For Surface Treatment Effects*, 2003.

[Lehocka et al. 2020] Lehocka, D. et al. "Effect of pulsating water jet disintegration on hardness and elasticity modulus of austenitic stainless steel AISI 304L," *The International Journal of Advanced Manufacturing Technology*, Vol. 107, No. 5–6, pp. 2719–2730, 2020. DOI: 10.1007/s00170-020-05191-3.

[Ma et al. 2021] Ma, Q. et al. "Experimental study on abrasive recycling in cutting with abrasive suspension water jet," *The International Journal of Advanced Manufacturing Technology*, Vol. 114, No. 3–4, pp. 969–979, 2021. DOI: 10.1007/s00170-021-06921-x.

[Martinec et al. 2002] Martinec, P. et al. *Abrasives for AWJ cutting*, Institute of Geonics, Academy of Sciences of the Czech Republic, Ostrava, 2002.

[Nadolny et al. 2017] Nadolny, K. et al. "SEM-EDS-based analysis of the amorphous carbon-treated grinding wheel active surface after reciprocal internal cylindrical grinding of Titanium Grade 2® alloy," *The International Journal of Advanced Manufacturing Technology*, Vol. 90, No. 5–8, pp. 2293–2308, 2017. DOI: 10.1007/s00170-016-9555-7.

[Nag et al. 2018] Nag, A. et al. "Hybrid aluminium matrix composite AWJ turning using olivine and Barton garnet," *International Journal of Advanced Manufacturing Technology*, Vol. 94, No. 5–8, pp. 2293–2300, 2018. DOI: 10.1007/s00170-017-1036-0.

[Oh et al. 2019] Oh, T.-M. et al. "Effect of Garnet Characteristics on Abrasive Waterjet Cutting of Hard Granite Rock," *Advances in Civil Engineering*, Vol. 2019, pp. 1–12, 2019. DOI: 10.1155/2019/5732649.

[Pavloušková et al. 2020] Pavloušková, Z. et al. “Characterization of High-Speed Alumina Abrasive Grinding Wheel,” *Defect and Diffusion Forum*, Vol. 405, pp. 365–369, 2020. DOI: 10.4028/www.scientific.net/DDF.405.365.

[Perec 2018] Perec, A. “Environmental Aspects of Abrasive Water Jet Cutting,” *Annual Set the Environment Protection - Rocznik Ochrona Srodowiska*, Vol. 20, No. 1, pp. 0258–0274, 2018.

[Perec 2021] Perec, A. “Research into the Disintegration of Abrasive Materials in the Abrasive Water Jet Machining Process,” *Materials*, Vol. 14, No. 14, pp. 3940, 2021. DOI: 10.3390/ma14143940.

[Perec et al. 2024a] Perec, A. et al. “Comparison of Chosen Metaheuristic Algorithms for the Optimization of the Abrasive Water Jet Treatment Process,” *MM Science Journal*, Vol. 2024, No. 5, pp. 7678–7686, 2024. DOI: 10.17973/MMSJ.2024_11_2024098.

[Perec et al. 2024b] Perec, A. et al. “Enhancing High-Alloy Steel Cutting with Abrasive Water Injection Jet (AWIJ) Technology: An Approach Using the Response Surface Methodology (RSM),” *Materials*, Vol. 17, No. 16, pp. 4020, 2024. DOI: 10.3390/ma17164020.

[Perec et al. 2025a] Perec, A. et al. “Multiple-Criteria Optimization of the Water Jet Cutting Process Using WISP Methodology,” In: *Advances in Water Jetting II*, Cham, 2025, pp. 122–133. DOI: https://doi.org/10.1007/978-3-031-72778-8_10.

[Perec et al. 2025b] Perec, A. et al. “AWJ Cutting Process Quality Modeling and Optimization Based on Footprint Angle,” *Materials*, Vol. 18, No. 24, pp. 5548, 2025. DOI: 10.3390/ma18245548.

[Perec, Musial 2021] Perec, A. and Musial, W. “Multiple Criteria Optimization of Abrasive Water Jet Cutting Using Entropy-VIKOR Approach,” In Hloch, S. et al. (eds.), *Advances in Manufacturing Engineering and Materials II*, Springer International Publishing, Cham, 2021, pp. 50–62. DOI: 10.1007/978-3-030-71956-2_5.

[Perec, Radomska-Zalas 2019] Perec, A. and Radomska-Zalas, A. “Modeling of Abrasive Water Suspension Jet Cutting Process Using Response Surface Method,” *AIP Conf. Proc.*, Vol. 2078, No. 020051, pp. 1–9, 2019. DOI: 10.1063/1.5092054.

[Prazmo et al. 2017] Prazmo, J. et al. “Abrasive grain disintegration during high-pressure abrasive water jet cutting in the abrasive reuse aspect,” *Conference on Water Jetting Technology: Water Jet 2017 – Research, Development, Application*, Ústav geoniky AV ČR, v. v. i. Ostrava, 2017, pp. 137–150.

[Praźmo et al. 2025] Praźmo, J. et al. “Influence of Abrasive Water Jet Cutting Parameters on the Surface Properties of Modern Plain Bearing Materials,” In: *Advances in Water Jetting II*, Cham, 2025, pp. 156–168. DOI: https://doi.org/10.1007/978-3-031-72778-8_13.

[Radomska-Zalas 2023] Radomska-Zalas, A. “Experimental Research on the Use of a Selected Multi-Criteria Method for the Cutting of Titanium Alloy with an Abrasive Water Jet,” *Materials*, Vol. 16, No. 15, pp. 5405, 2023. DOI: 10.3390/ma16155405.

[Riha et al. 2021] Riha, Z. et al. “Comparison of the disintegration abilities of modulated and continuous water jets,” *Wear*, Vol. 478–479, pp. 203891, 2021. DOI: 10.1016/j.wear.2021.203891.

[Szatkiewicz et al. 2023] Szatkiewicz, T. et al. “Preliminary Studies into Cutting of a Novel Two Component 3D-Printed Stainless Steel–Polymer Composite Material by Abrasive Water Jet,” *Materials*, Vol. 16, No. 3, pp. 1170, 2023. DOI: 10.3390/ma16031170.

[Varga et al. 2023] Varga, M. et al. Impact-abrasive wear resistance of high alumina ceramics and ZTA, 2023. DOI: 10.21203/rs.3.rs-2440544/v1.

[Zaremba et al. 2015] Zaremba, D. et al. “Particle Disintegration in the Abrasive Water Injection Jet,” *2015 WJTA-IMCA Conference and Expo Proceedings*, WJTA-IMCA, New Orleans, Louisiana, USA., 2015, pp. Paper D3.

CONTACTS:

Prof. Dr. Ing. Andrzej Perec, D.Sc.
AJP University, Faculty of Technology
Chopina 52, Gorzow Wlkp, 66-400, Poland
+48 95 7279536, aperec@ajp.edu.pl

LICENSE CREATIVE COMMONS: